ELSEVIER

Available online at www.sciencedirect.com

SCIENCE DIRECT®

Coordination Chemistry Reviews 250 (2006) 1696–1709

COORDINATION CHEMISTRY REVIEWS

www.elsevier.com/locate/ccr

Review

Raman scattering and photophysics in spin-state-labile d^6 metal complexes

Wesley R. Browne[a], John J. McGarvey[b,*]

[a] *Organic and Molecular Inorganic Chemistry, University of Groningen, Groningen, The Netherlands*
[b] *School of Chemistry and Chemical Engineering, Queen's University Belfast, Northern Ireland, Belfast BT5 9AG, UK*

Received 8 September 2005; accepted 12 January 2006

Contents

Abstract

In this review two areas of d^6 transition metal ion chemistry and photophysics are briefly reviewed (i) that of Ru(II)dipyridophenazine (dppz) complexes as DNA intercalators and (ii) spin crossover behavior in Fe(II) complexes. In both areas the role of Raman spectroscopy in providing information concerning the spectroscopy and photophysics of the electronic states involved and the interactions between states of differing spin multiplicity is discussed.

Keywords: d^6 transition metal ions; DNA-intercalating metal complexes; Light-switch effect; Resonance Raman scattering; Spin-crossover complexes

1. Introduction

The remarkable variation in the photophysical properties of the d^6 transition metal ions Fe(II) and Ru(II) has been recognized from the 1970's and earlier.[1] An important factor is the ligand field around the metal ion. For intermediate fields in d^6 iron(II) complexes spin crossover (SCO) behavior is of interest whilst for the strong field d^6 ruthenium(II) complexes luminescence from charge transfer states dominates. Vibrational spectroscopy is an especially useful tool for exploring the changes in molecular structure, particularly the bond length changes which characterize the rather different behaviour of the two groups. In the present review we will discuss two important areas in which Raman spectroscopy has proven to be a useful tool for structural elucidation: DNA interactions with Ru(II) polypyridine complexes, and the spin crossover phenomenon observed in Fe complexes. No attempt is made at comprehensive coverage of either of these topics. Instead, selected examples have been chosen to illustrate Raman scattering as the basis of informative probe techniques of ground and excited states in both areas.

---

* Corresponding author. Tel.: +44 28 9097 5450; fax: +44 28 9097 4890.
E-mail address: j.mcgarvey@qub.ac.uk (J.J. McGarvey).

0010-8545/$ – see front matter © 2006 Elsevier B.V. All rights reserved.
doi:10.1016/j.ccr.2006.01.009

1.1. d^6 metal ions

The lack of optically excited states with long lifetimes among Fe(II) coordination compounds, (the latter having instead low energy ligand field (LF, or dd) states associated with radiationless relaxations back to the ground state through sub-nanosecond or indeed sub-picosecond [2] intersystem crossing (ISC) and internal conversion (IC) processes), prompted the comment in an important 1994 review by Guetlich, Hauser and Spiering [3], that Fe(II) complexes:

> ‘have had a comparatively [lowly] standing compared to other transition metal complexes in regard to the study of their photophysical and photochemical properties’

The group VIII (i.e. Fe, Ru, Os) transition metal elements and their cations have dominated the area of transition metal supramolecular chemistry, since the 1960’s and 70’s [4,5]. In particular, ruthenium(II) complexes display versatile photophysical properties, leading to intense interest in potential applications in photo-molecular devices [6], photocatalysis [4], and artificial photosynthesis [7]. This has been to a large extent due to the varied character of their emissive excited states, which are generally long lived and undergo not only luminescence but also photochemistry, excited state electron transfer and photo-oxidation and -reduction as well as energy transfer processes [4,6]. The basic ligand field model for a transition metal complex and the possible orbital transitions, which may occur, are shown in Fig. 1. In reality, while such diagrams do not describe the electronic structure of transition metal complexes very well, they do serve to illustrate the transitions responsible for the electronic absorption spectra of polypyridyl complexes, of d^5 and d^6 metal ions in particular.

The four transitions shown in Fig. 1 are:

(1) Ligand centred (LC) or intraligand (IL) are equivalent to that observed for the free ligand.
(2) Metal to ligand charge transfer (MLCT) where the metal centre is formally oxidised and the ligand reduced.
(3) Metal centered (MC or dd): a transition from the formally non-bonding t_{2g} to the anti-bonding e_g orbitals.

Table 1
Lowest excited states of $[M^{II}(bpy)_3]^{2+}$ complexes

Metal complex	Lowest excited state	Luminescence (λ_{max})
$[Fe(bpy)_3]^{2+}$	^{3}MC	Absent
$[Ru(bpy)_3]^{2+}$	^{3}MLCT	Intense (610 nm at 298 K)
$[Os(bpy)_3]^{2+}$	^{3}MLCT	Weak (720 nm at 298 K)

(4) Ligand to metal charge transfer (LMCT) where the ligand is oxidised and the metal reduced.

Other transitions not shown in Fig. 1 are ligand-to-ligand (LLCT) and metal-to-metal charge transfer (MMCT). These transitions will not be considered further in the present review.

The intense red colour of the Fe(II) complex with 2,2′-bipyridyl, $[Fe(bpy)_3]^{2+}$ is due to strong absorption in the visible spectrum. However, the complex is not luminescent and its lowest excited state is ligand field (^{3}MC) rather than charge transfer in nature, rendering it inherently photochemically unstable. Osmium analogues, in contrast, exhibit chemistry closely related to that of ruthenium, although for $[Os(bpy)_3]^{2+}$ the ^{3}MLCT excited state lifetime is 10–30 times shorter than for $[Ru(bpy)_3]^{2+}$. The ^{3}MC state of $[Os(bpy)_3]^{2+}$ lies at higher energy than that of $[Ru(bpy)_3]^{2+}$, and for this reason, osmium complexes are photochemically inert. The effect of metal substitution on the lowest excited state and on the emission energy of a series of bpy-based complexes is shown in Table 1.

The electronic state manifolds of $[M^{II}(bpy)_3]^{2+}$ (M = Fe, Ru, Os) are illustrated in Fig. 2. For low spin M^{II} complexes the ground electronic state is of singlet multiplicity, hence only transitions to singlet-excited states are formally allowed. For Os(II) and to a lesser extent Ru(II), transitions to the ^{3}MLCT states are observable in the visible region of the UV–vis absorption spectra as a result of spin–orbit coupling.

2. Application of Raman and resonance Raman spectroscopy in elucidating electronic and molecular structure

The application of Raman spectroscopy to the study of d^6 transition metal complexes has been dominated by investigations

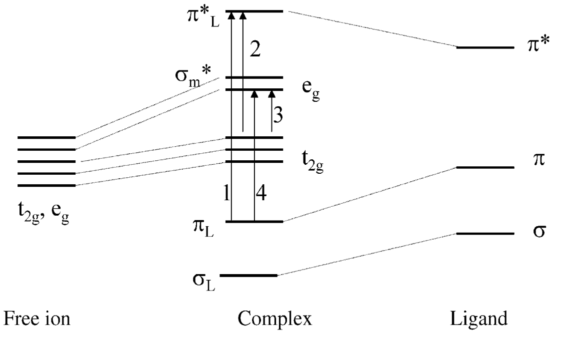

(1) ππ* (LC); (2) dπ* (MLCT); (3)dd* (MC); (4) πd* (LMCT)

Fig. 1. Energy level diagram showing the relative disposition of metal and ligand orbitals and possible electronic transitions for a transition metal complex in an octahedral ligand field.

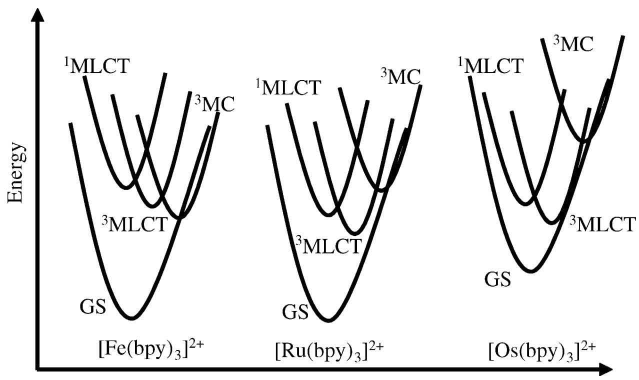

Fig. 2. Ground and excited state PE curves for $[M^{II}(bpy)_3]^{2+}$ complexes (M = Fe, Ru, Os).

of Ru(II) polypyridyl systems, in part due to the pioneering work of Kincaid and others on the paradigm complex, $[Ru(bpy)_3]^{2+}$ [8].

The paper by Woodruff and Dallinger, published just over 25 years ago [9], describing the use of a single nanosecond laser pulse to populate the lowest ^{3}MLCT state of $[Ru(bpy)_3]^{2+}$ and to probe the resonantly enhanced Raman scattering from that state (a technique known as transient resonance Raman (or TR^2) spectroscopy) was the first application of such an approach to the investigation of a metal-centered excited state species. That paper provided the impetus for a flurry of applications of the technique to metal-centered systems over the next couple of decades. There are now many instances in the literature of the effectiveness of both TR^2 and TR^3 (time-resolved resonance Raman, involving separate time-sequenced laser pulses as pump and probe) for elucidation of the vibrational structure of the excited states of metal complexes. An attractive feature of the techniques is their versatility of application in both homogeneous solvents, aqueous and non-aqueous [10,11], and in microheterogeneous environments such as colloids, gels or micelles [12]. Notwithstanding the title of the present article, it is not the intention here to provide a comprehensive review of the application of TR^2 and TR^3 to metal complex excited states and transients. The field has already been reviewed, at least for the period up to ca. 1998 [e.g. 10,11,13] and there has been a short account recently of further examples [14].

The intention here is rather to present a brief survey of recent studies by both ground state and transient/time-resolved Raman spectroscopy of some complexes of d^6 metal ions which have attracted interest for the reasons already mentioned: complexes which function as light–switches towards DNA and complexes exhibiting the phenomenon of electronic spin state crossover.

In practice, with regard to interactions with DNA, attention will be limited to complexes of Ru(II), Os(II)and Re(I) and within this group, the main focus will be on complexes with the ligand dipyridophenazine (dppz), which became the centre of a great deal of attention both on account of its intercalative ability towards DNA and the DNA 'light–switch' (vide infra) properties of the complexes $[M(L)_2dppz]^{2+}$ (L = 2,2′-bipyridyl (bpy); 1,10-phenanthroline (phen)) and with various substituted dppz ligands. So far as dppz and related ligands are concerned, the d^6 metal ions of primary interest are Ru(II), Os(II) (the latter to a much more limited extent) and Re(I). In the case of Fe(II), although complexation with the dppz ligand has been reported, namely in the complex $[Fe(dppz)_2(NCS)_2]$, the interest in that instance was on the spin crossover properties of the complex [12a,15], an area discussed in Section 4.

3. Probing DNA interactions by Raman scattering techniques

Transition metal photochemistry and spectroscopy have been enriched continually over several decades by the search for new molecular probes, particularly in the bio-inorganic field, and in the development of optically driven devices and sensors. One area on which considerable attention has been focused concerns complexes capable of selectively binding to nucleic acids. Although the Ru(II) complexes, $[Ru(L)_2dppz]^{2+}$, with the planar aromatic ligand, dppz, (where L = 1,10-phenanthroline (phen) or 2,2′-bipyridyl (bpy) have been known for almost two decades as nucleic acid probes and in particular for their so-called 'light–switch' properties towards DNA, they have remained the subject of frequent spectroscopic, photophysical and more recently, theoretical enquiry.

The general account of the 'light–switch' effect is well known and the broad basis of the phenomenon agreed and it has been described in terms such as the following, by numerous authors [16,17]. In summary, $[Ru(L)_2dppz]^{2+}$ exhibits a very weak, virtually undetectable ^{3}MLCT luminescence in aqueous solution, which is enhanced (by more than four orders of magnitude in the case of $Ru(phen)_2dppz]^{2+}$) [18] in the presence of DNA and in a range of non-aqueous solvents. The effect in DNA is ascribed to intercalative binding of the ligand between the base pairs of DNA, the extended, planar aromatic surface of the ligand allowing for extensive hydrophobic $\pi\pi$ stacking between base pairs and resulting in a decrease in efficiency of non-radiative relaxation from the MLCT excited state [17b–d].

In the present review, attention is directed primarily to contributions which Raman and resonance Raman scattering techniques, both CW and time-resolved, have made to the area, the discussion being set in the context of other relevant investigations. The DNA 'link' referred to above has been responsible in large measure for the sustained interest in the dppz ligand and its transition metal complexes. It is not surprising that the potential of resonance Raman spectroscopy as a structural probe in this area, with its inherent ability to discern changes in ligand vibrational mode patterns associated with specific electronic (vibronic) transitions, was recognized soon after the first reports of the light–switch properties of $[Ru(bpy)_2dppz]^{2+}$ and analogues. Two broad issues have been of primary concern: the electronic nature of the lowest excited states of the complexes and the underlying photophysical mechanism of the light–switch effect.

3.1. *Electronic structure of low-lying excited states in $[Ru(L)_2dppz]^{2+}$*

Cyclic voltammetry, UV–vis and EPR studies of dppz and the complex $[Ru(bpy_2dppz]^{2+}$ by Kaim et al. [19] identified three low-lying MO's described as phenazine-type (lowest in energy) and the b_1 and a_2 orbitals located on the bpy part of the dppz ligand. Occupation of the phenazine-type MO via MLCT excitation leads to the possibility of electrophilic addition at the phenazine nitrogens but steric considerations confine access to protons, as electrophiles. This selectivity for emission quenching proton in an already partly hydrophobic heteroaromatic pocket was regarded [19] as crucial for the light–switch operation of the Ru complex, succinctly described by Kaim et al. as a 'water-induced luminescence quenching in hydrophobic microenvironments'.

In early studies, [20] it was suggested that in the ^{3}MLCT state reached upon photo-excitation of $[Ru(bpy)_2dppz]^{2+}$ the electron was localized on the phenazine part of dppz. However, the extent of coupling between the phenazine radical anion and the (formally) Ru^{III} centre remained somewhat loosely defined. The issue was addressed in an important communication by

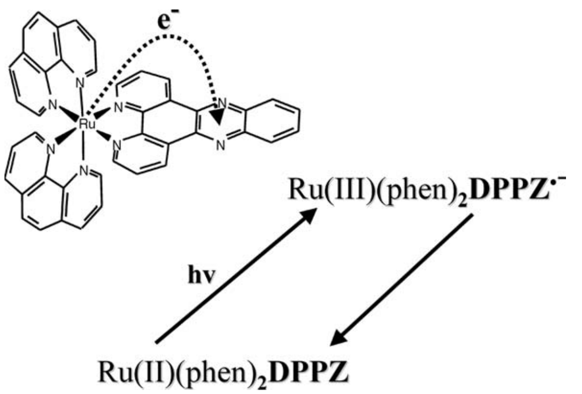

Fig. 3. $[Ru(phen)_2dppz]^{2+}$ and schematic representation of a MLCT state.

Schoonover, Bates and Meyer [21] using CW and transient resonance Raman (rR) techniques at several probe wavelengths spanning the intraligand and MLCT transitions of $[Ru(bpy)_2dppz]^{2+}$ and $[Ru(dimethylbpy)_2dppz]^{2+}$. For both complexes, the excited state RR spectra revealed dppz as the acceptor ligand (Fig. 3). Significantly, no vibrational bands for $bpy^{\bullet -}$ or $dmb^{\bullet -}$ were detected. Instead, the bands observed displayed a pattern similar to that for the $dppz^{\bullet -}$ radical anion, prepared electrochemically, i.e. the populated excited state was formulated as $[Ru^{III}(L)_2dppz^{\bullet -}]^{2+}$ (L = 1 bpy or dmb). Furthermore, it was pointed out that the vibrational band pattern could be viewed as a superposition of $phen^{\bullet -}$ radical anion and phenazine modes.

This was presented as a reasonable proposal, given the structures of phen and dppz, but only if the excited electron were regarded as being partly delocalized over the entire dppz framework. A very important observation underlined by Schoonover et al. [21], consistent with partial delocalization, is that the extent of resonance enhancement and observed frequency shifts for the phenazine bands in the excited-state spectra are small relative to those for phenazine and its own radical anion.

An additional point addressed by Schoonover et al. is the question of the relative ordering of the low-lying dppz-based (^{3}MLCT and $^3\pi\pi^*$) excited states in Re(I) dppz complexes, a matter which also bears on other transient resonance Raman studies of $[Ru(L)_2dppz]^{2+}$ complexes, *vide infra*.

Single color excited state resonance Raman measurements carried out on the complexes *fac*-$[Re(dppz)(CO)_3(PPh_3)]^+$ and *fac*-$[Re(dppz)(CO)_3Cl]$ in CH_2Cl_2 at room temperature yielded identical sets of spectra, broadly similar to, but differing in precise detail from, the pattern for the $Ru^{III}(dppz^{\bullet -})$ MLCT excited states referred to above. For the PPh_3 complex, emission and excited state infrared studies supported a lowest energy, dppz-centred $^3\pi\pi^*$ state. Spectral comparisons show that the lowest state in *fac*-$[Re(dppz)(CO)_3Cl]$ at room temperature is also $^3\pi\pi^*$, despite the occurrence of emission arising from a ^{3}MLCT state.

In a related context, Gordon et al. [22,23] have investigated the states formed upon photoexcitation of Cu(I) and Re(I) complexes of dppz and a number of substituted analogues of this ligand. Using a combination of resonance Raman spectroelectrochemistry, transient resonance Raman and excited state absorption techniques, it was shown that the lowest excited state was dppz-centred $^3\pi\pi^*$, except where an electron-withdrawing substituent was present on the dppz. As already alluded to above, the situation regarding excited state ordering in Re(I) complexes of the type under consideration here can be subtle. Time-resolved infrared (TRIR) spectroscopy is an important tool in this regard, and the area has been well reviewed [24].

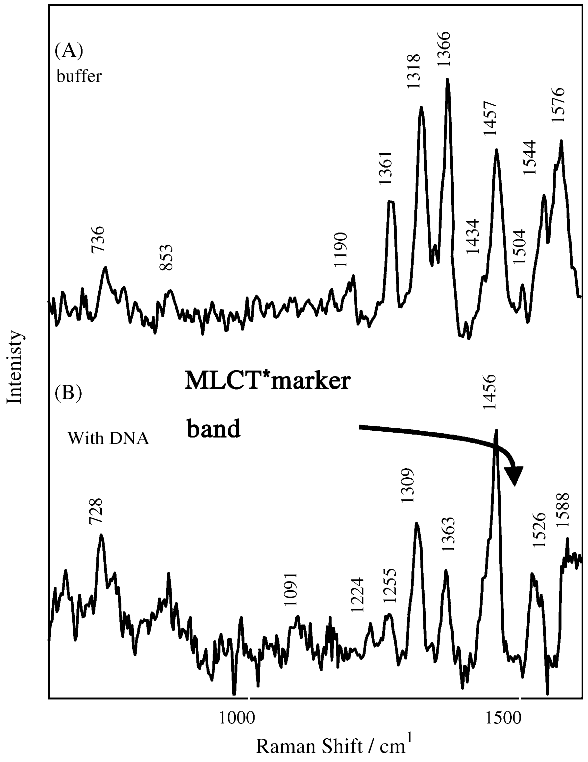

Fig. 4. TR^2 spectra of $[Ru(phen)_2dppz]^{2+}$ in buffer solution and in DNA(λ_{ex} = 355 nm, pulsed excitation).

Recent studies of the excited state properties of *fac*-$[Re(CO)_3(dppz)(py)]^+$ in acetonitrile using a series of complementary techniques including visible and infrared transient absorption and time-resolved resonance Raman spectroscopy and TRIR on picosecond and nanosecond timescales demonstrated that the lowest-lying emissive state in this complex is also $^3\pi\pi^*$, localized on the dppz ligand; this multi-technique based study also provided detailed information on the dynamics following photo-excitation [25]. The TR^3 spectra reported in this investigation provide a good demonstration of how dppz-localized ^{3}MLCT and $^3\pi\pi^*$ states can be readily distinguished by the resonance Raman approach. The spectra in Fig. 4, when compared with those in Fig. 5, illustrate the point.

3.2. Probing the interaction between Ru(II) complexes and DNA by resonance Raman spectroscopy

An early instance of the use of transient rR methods in the general area under consideration here appeared in a paper [12c] describing single color TR^2 studies of the MLCT excited states of $Ru(dmb)_2dppz$ in micelle and DNA environments, but the first transient resonance Raman studies to focus specifically on the light–switch interaction of dppz complexes towards DNA

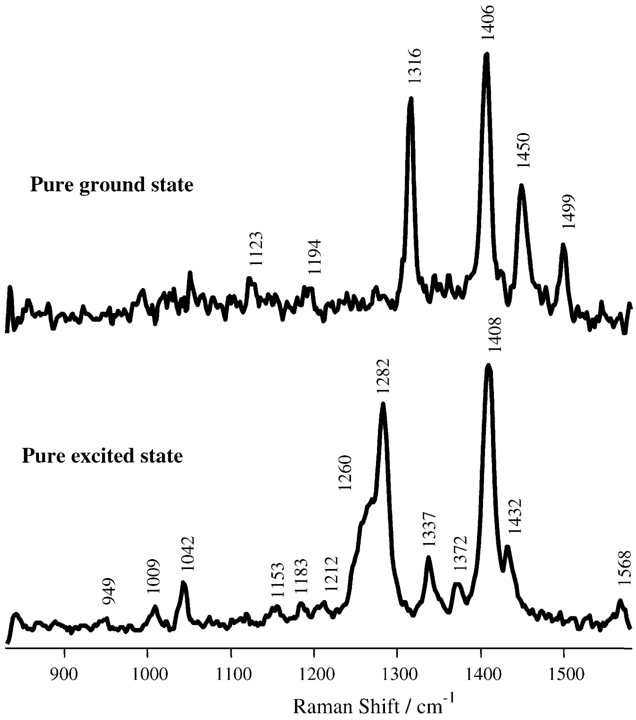

Fig. 5. Pure ground and excited state spectra of [Re(CO)$_3$dppz.py] in CD$_3$CN obtained from ns-TR^3 (450 nm probe/355 nm pump). No ^{3}MLCT (dppz$^{\bullet-}$) features are observed, however, the features near 1280 and 1408 cm^{-1} are characteristic of a $^3(\pi\pi^*)$ ^{3}IL state. Reproduced from Ref. [25] with permission of the Royal Society of Chemistry. Copyright RSC 2003.

appeared in a short communication in 1996 [27] followed soon after by a more extensive report [28]. These papers describe resonance-Raman spectroscopy coupled with flash photolysis techniques to probe the interaction between the complexes [RuL$_2$(dppz)]$^{2+}$ (L = phen or bpy) and calf-thymus DNA. The transient studies were paralleled by CW investigations.

Acquisition of ground electronic state rR spectra using CW excitation is generally an essential counterpart to excited state rR studies and is particularly the case in the present instance where investigations have necessarily been conducted in several types of media, aqueous buffer, DNA and non-aqueous solvent. A thorough study of the ground state rR spectroscopy of both [Ru(phen)$_2$dppz]$^{2+}$ and [Ru(bpy)$_2$dppz]$^{2+}$ at several excitation wavelengths has been reported [28], together with complementary UV–vis measurements, both studies carried out in buffer and in DNA.

Changes in the enhancement patterns of the ground-state resonance-Raman spectra of both complexes in the presence of DNA are consistent with changes to the UV–vis absorption spectrum (Fig. 6). Intensity changes in the rR spectra recorded at 457.9 nm were shown to be the result of a lowering in intensity of the dppz component of the ^{1}MLCT absorption in the presence of DNA. At 363.8 nm, larger changes occurring in the rR spectra were noted (Fig. 7), paralleling the larger changes in the UV–vis in this region. The most marked changes, which occur are in modes associated with the intercalating dppz ligand.

In the absence of DNA, it is apparent [28] on switching from 457 to 488 nm excitation that the relative intensities of dppz

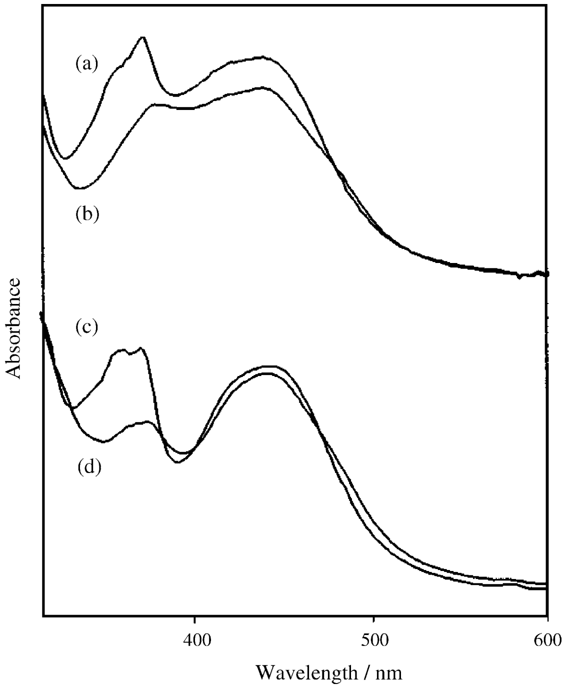

Fig. 6. UV–vis spectra of [Ru(phen)$_2$(dppz)]$^{2+}$ (a and b) and [Ru(bpy)$_2$(dppz)]$^{2+}$ (c and d): (a and c) in buffer; (b and d) [DNAphosphate]:[Ru] ratio of 20:1. Reprinted with permission from Ref. [28]. Copyright [1997] American Chemical Society.

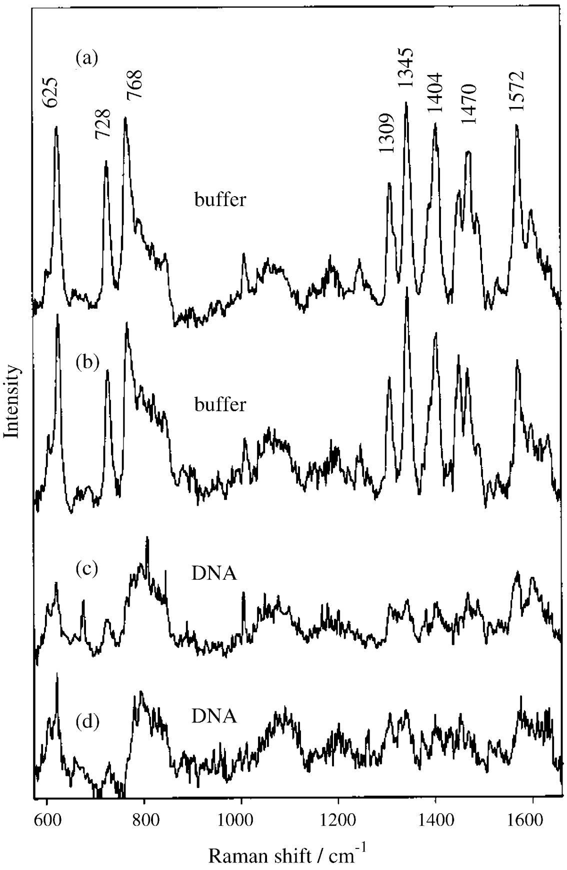

Fig. 7. Ground state RR spectra of [Ru(phen)$_2$(dppz)]$^{2+}$ (a and c) and of [Ru(bpy)$_2$(dppz)]$^{2+}$ (b and d) recorded at λ_{ex}) 363.8 nm: (a and b) in buffer; (c and d) [DNA-phosphate]:[Ru] ratio of 20:1. Reprinted with permission from Ref. [28]. Copyright [1997] American Chemical Society.

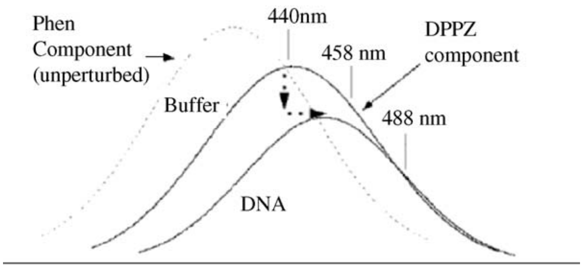

Fig. 8. The enhancement patterns observed in the ground state RR spectra at each probe wavelength in the presence and absence of DNA suggest a lowering of intensity coupled with a red shift of the dppz component of the MLCT absorption upon intercalation, represented schematically here. Reprinted with permission from Ref. [28]. Copyright [1997] American Chemical Society.

features increase with respect to phen features, suggesting that the degree of resonance enhancement of dppz vibrational modes becomes greater at longer wavelengths. Further, it is clear that a lowering in intensity of dppz features with respect to phen features occurs upon DNA addition, but the extent of this effect evidently decreases toward longer probe wavelengths.

The enhancement patterns observed in the ground state rR spectra at each probe wavelength in the presence and absence of DNA suggest a lowering of intensity coupled with a red shift of the dppz component of the MLCT absorption upon intercalation, represented schematically in Fig. 8.

The findings illustrate the ability of rR spectroscopy to selectively probe ligand vibrational modes even where spectral overlap might be a compromising feature.

In the same investigation, [28] transient rR spectra of the complexes $[Ru(phen)_2dppz]^{2+}$ and $[Ru(bpy)_2dppz]^{2+}$, both in aqueous buffer and in DNA, showed several modes (Fig. 9) attributable to coordinated $dppz^{\bullet-}$ radical anion, reflecting population of the MLCT excited state $[Ru^{III}(L)_2dppz^{\bullet-}]^{2+*}$ within the duration of the 8 ns laser pulse, in agreement with the earlier studies [21] referred to above. Significant changes are evident when DNA is present.

In a paper, [26] which appeared almost simultaneously with this study, results of an analogous resonance Raman investigation of $[Ru(phen)_2dppz]^{2+}$ were interpreted, in contrast, as consistent with the population of a dppz-centered $^3\pi\pi^*$ state upon photoexcitation. A subsequent commentary argued against this [29], suggesting that the divergence of opinion over the nature of the lowest excited state of ruthenium(II) dppz complexes finds a resolution through consideration of spectral data for rhenium-(I) dppz complexes, for which there is known to be a close interplay between $\pi\pi^*$ (ligand-centered) and MLCT excited states. The relevant transient Raman data [21] show that while bands due to $[Re(dppz)(CO)_3(PPh_3)]^+$ and $[Re(dppz)(CO)_3Cl]$ fall in very much the same frequency ranges as those reported for the Ru(dppz) complexes, closer scrutiny reveals differences in detail from the pattern reported for $Ru^{III}(dppz^{\bullet-})$

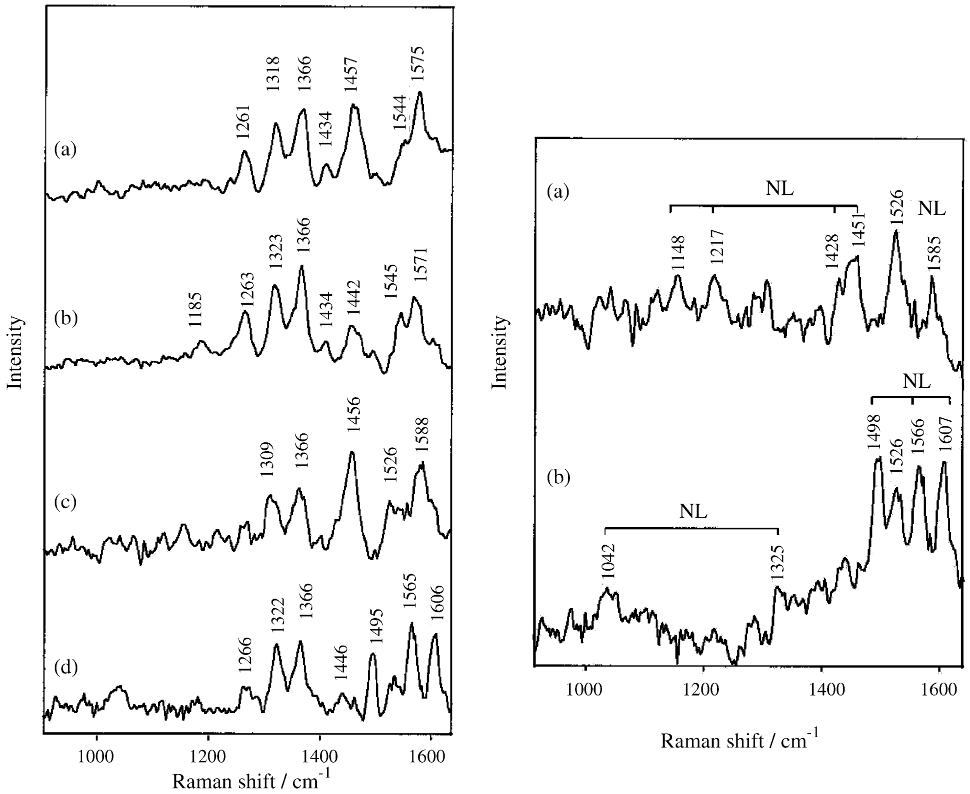

Fig. 9. Left: Excited state resonance Raman spectra of $[Ru(phen)_2(dppz)]^{2+}$ (a and c) and $[Ru(bpy)_2(dppz)]^{2+}$ (b and d) recorded with the single color laser pulse method (laser pulse duration ca. 8 ns, at λ_{ex} 355 nm, pulse energy was such that essentially 100% conversion was achieved): (a and b) in buffer; (c and d) [DNA phosphate]:[Ru] ratio of 20:1. Right: scaled subtractions of spectra shown in (left) [spectra recorded in the presence of DNA]—[spectra recorded in aqueous buffer solution] of (a) $[Ru(phen)_2(dppz)]^{2+}$ and (b) $[Ru(bpy)_2(dppz)]^{2+}$. Each subtraction is scaled for complete removal of the 1366 cm^{-1} $dppz^{\bullet-}$ feature. NL denotes neutral ligand modes of the corresponding ancillary ligands. Reprinted with permission from Ref. [28]. Copyright [1997] American Chemical Society.

excited states. Importantly, for [Re(dppz)$(CO)_3Cl$], the TR^2 spectrum is different from the rR spectrum of the reduced complex [Re($dppz^{\bullet -}$)$(CO)_3Cl$], which exhibits bands at 1363 and 1456 cm^{-1}, [23] close to those observed in the TR^2 spectrum of ruthenium(II) dppz complexes, in all three investigations referred to above, [21,27,28] and consistent with assignment of the latter spectrum to $dppz^{\bullet -}$. This more generally held view of an MLCT excited state receives further support from more recent TR^3 investigations [30,31]. In addition, variable temperature luminescence measurements [16,32] (*vide infra*) on $[Ru(bpy)_2dppz]^{2+}$ confirm that a dppz-centered $^3\pi\pi^*$ state does not play a significant role in the emissive behaviour of this complex in fluid solvents.

The initial TR^2 studies [27,28] of $[Ru(phen)_2dppz]^{2+}$ and $[Ru(bpy)_2dppz]^{2+}$ in the presence of DNA also revealed a band near 1526 cm^{-1}, assigned as a mode of the $dppz^{\bullet -}$ anion and linked to the intercalative interaction of the dppz ligand with the binding sites of DNA (Fig. 4 above). The appearance of this feature was confirmed in later work [30,31]. Aside from it being a convenient marker band for intercalation per se [28], the relative intensity of the band was shown to depend also upon the enantiomeric form of Ru(II) complex bound to the DNA, thus rendering it in effect a marker of the distinctive response of the Δ and Λ enantiomers to the DNA binding sites as well [28]. Significantly, further studies [38] with the d_6-isotopomer of the dppz ligand enabled assignment of this 1526 cm^{-1} band to the phen region of the dppz ligand, i.e. attributable to a normal mode of vibration enhanced via resonance with a $dppz^{\bullet -}$ intraligand electronic transition of an MLCT state with increased charge density on the phen segment of the reduced ligand [38]. This has further significance in regard to the light–switch mechanism itself but first it is necessary to take a closer look at the photophysics of the phenomenon.

3.3. Light–switch photophysics

The early reports of the light–switch effect exhibited by $[Ru(phen)_2dppz]^{2+}$ and its utility as a probe of DNA prompted a detailed study [33] of the photophysics of the complex in aqueous and non-aqueous media by time-resolved absorption and emission spectroscopy on picosecond and nanosecond timescales. In essence, this was an investigation into the photophysical response of the complex to the solvent environment, leading to the proposal of a possible mechanism for the light–switch effect involving two close-lying MLCT states, both dppz-based, of triplet character, (formally $[Ru^{III}(phen)_2dppz^{\bullet -}]^{2+}$), with relative energies sensitive to the polarity of the solvent environment and denoted *MLCT*$^{/}$ and *MLCT*$^{//}$, referred to later also as 'bright' (B) and 'dark' (D), respectively. A unified photophysical model for water and acetonitrile was proposed on the basis of this investigation and is shown in Fig. 10.

In summary, following fast (<300 fs) photogeneration in either solvent of the charge-transfer state (*MLCT*$^{/}$), the scheme in Fig. 10 (LHS) for water proposes ultrafast (ca. 3 ps) internal conversion to *MLCT*$^{//}$, which decays rapidly (250 ps) and non-radiatively to the ground state. In acetonitrile by contrast, (and, by presumed [33] extension of the scheme, in DNA also) it was proposed that the MLCT$^{//}$ state is located sufficiently high in energy relative to MLCT$^{/}$ (Fig. 10, RHS), as to preclude its population; thus intense luminescence from MLCT$^{/}$ becomes the dominant photophysical process. The influence of the solvent environment on the luminescence spectroscopy and photophysics of $[Ru(phen)_2dppz]^{2+}$ has also been investigated in some detail [34].

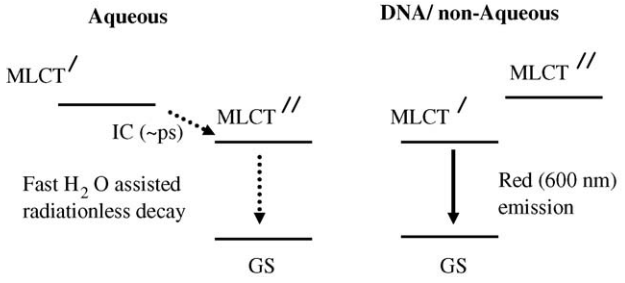

Fig. 10. A unified photophysical model for water and acetonitrile as proposed by Olson et al. Reprinted with permission from Ref. [33]. Copyright [1997] American Chemical Society.

The environment-sensitive model proposed on the basis of the time-resolved absorption and luminescence investigation by Barbara et al. [33] triggered time-resolved resonance Raman studies spanning similar timescales [30,31] (i.e. from a few ps to 100's of ps) and a further study [35] over a less extended timescale, out to ca. 20 ps (Fig. 11). The first two studies included investigations in DNA, in addition to studies in water and acetonitrile. Vibrational marker features and enhancement patterns [30] signaled rapid progression (<20 ps) between two triplet MLCT states in aqueous environment, followed by subnanosecond, non-radiative deactivation to the ground state. In non-aqueous environment, the long-lived, emissive triplet MLCT state was spectrally identified as the short-lived (bright) first triplet MLCT state, *MLCT*$^{/}$, observed in water, in agreement with the earlier proposed mechanism [33] (Fig. 10). An additional feature, not reported in the earlier photophysical study, was the observation [30,31] in all media, aqueous, non-aqueous and DNA, of a 'precursor' state preceding *MLCT*$^{/}$, as depicted in the scheme above. It has been speculated [31] that the

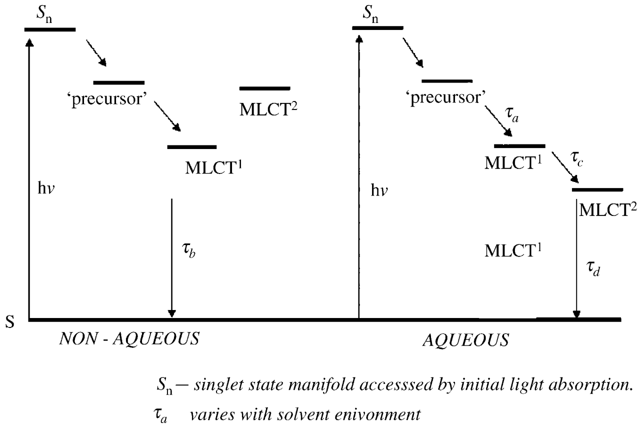

Fig. 11. Schematic photophysical diagram for $[Ru(phen)_2dppz)]^{2+}$ Reprinted with permission from Ref. [30]. Copyright [2001] American Chemical Society.

precursor could be regarded as the Franck–Condon manifold ‘state’ of $[Ru(phen)_2dppz]^{2+}$, consisting of ^{1}MLCT states localized on any one of the three ligands, with subsequent, ultrafast (<100 fs) conversion to the corresponding localized ^{3}MLCT states being followed by interligand electron transfer to yield the final, dppz-localized ^{3}MLCT state.

The data from these picosecond TR^3 studies were shown to correlate well with previous nanosecond RR findings [27,28] for the complex in each environment. Moreover, it proved possible [30] to use the 1526 cm^{-1} marker band to follow the early stages of excited state development in water. Thus, the 1526 cm^{-1} feature can be correlated with the ‘bright’ MLCT$^{/}$ state, which is characterized by an electron density, which is polarized more toward the phenanthroline segment of the dppz ligand, compared to the MLCT$^{//}$ state, for which no enhancement of the 1526 cm^{-1} feature is observed. This in turn is consistent with a model involving increased stabilization in the polar water environment of the MLCT$^{//}$ state, which has been proposed to have more electron density on the “phenazine” nitrogens, relative to MLCT$^{/}$, and which would facilitate efficient non-radiative decay to the ground state.

Although the two-state model [33] for the light–switch effect receives general support from the TR^3 studies and it was already clear from the latter studies [30] that the excited state spectra in a variety of media, including MeCN, MeOH and DNA are quite distinct, suggesting that solvation is a significant factor [31], the precise role of solvent in the mechanism has been the subject of much closer scrutiny in several later papers [16,32,36,37].

Using single photon counting in the picosecond range, two groups have studied the temperature dependence of the emission for $[Ru(phen)_2dppz]^{2+}$ in several polyol solvents including glycerol [36,37] and for $[Ru(bpy)_2dppz]^{2+}$ in aprotic (nitrile) and protic media [16,32]. Both groups report an anomalous temperature dependence of emission lifetimes and quantum yields, compared to the well-known normal monotonic dependence for Ru(II)polypyridyl complexes. For $[Ru(bpy)_2dppz]^{2+}$ in nitrile solvents the emission lifetime reached a maximum with decreasing temperature and subsequently decreased with further lowering of temperature. The findings were interpreted in terms of a dynamic equilibrium between two MLCT states, ‘bright’ (B) and ‘dark’ (D) both localized on the dppz ligand but differentiated as ‘phenazine-like’ (D) and ‘bpy-like’ (B). Although supporting the involvement of two states in the light–switch mechanism, the observed data were considered [16] to be inconsistent with solvent-induced state reversal as proposed previously [33], instead pointing to a scheme in which the D state remained lowest in energy in all solvents, with competing enthalpic factors favoring the D state and entropic factors favoring the B state. A broadly equivalent picture has been advanced [36,37] to explain the findings for $[Ru(phen)_2dppz]^{2+}$ in glycerol and other polyol solvents, with an equilibrium between a dark (non- or weakly emissive) state(s) involving solvent H-bonding to one or both phenazine nitrogens and a bright, emissive, non-hydrogen bonded state. Thus, in essence the light–switch mechanism itself is dictated by the thermodynamics of an equilibrium between B and D states, although the kinetics of the equilibrium do of course remain relevant to the photophysics of the light–switch. Single-exponential decay kinetics were observed at all temperatures, consistent with a constant equilibrium between B and D [32]. The results from the ultra fast TR^3 experiments [30,31] referred to earlier support the concept of a fast interconversion between these two states. It was suggested that the interconversion time (<20 ps) between MLCT$^{/}$ (≡‘B’) and MLCT$^{//}$ (≡‘D’) reported in the TR^3 studies could correspond to the time it takes to establish the equilibrium populations.

Closer examination of the basic ideas expressed in both groups of investigations concerning the nature of the MLCT excited states implicated in the light–switch phenomenon reveals a considerable level of support in the results of TR^3 studies, concerning the electronic nature of these states. Significantly, both groups view the bright state as photophysically akin to the respective $[Ru(L)_3]^{2+}$ (L = bpy or phen) complexes, i.e. localised on the ‘bpy’ or ‘phen’ dppz fragment remote from the phenazine segment. The results of TR^2 experiments [38] in which comparisons were made between the transient rR spectra of $[Ru(phen)_2dppz]^{2+}$ containing the natural abundance dppz (h_{10}) ligand and the dppz ligand with the phen fragment deuteriated (i.e. d_6) provide a clear indication that the prominent mode at 1526 cm^{-1} characterising the B state observed in the initial TR^2 studies [28] for both $[Ru(phen)_2dppz]^{2+}$ and $[Ru(bpy)_2dppz]^{2+}$ and confirmed subsequently [30,31], is indeed localised on the ‘phen/bpy’ fragment of the dppz ligand. This experimental confirmation of the nature of the bright state may have been overlooked previously [39].

The structurally similar complex $[Ru(tap)_2dppz]^{2+}$ (tap = 1, 4,5,8 tetraazaphenanthrene), which intercalates with DNA via the dppz ligand has also been investigated [40] by transient resonance Raman on nanosecond timescales and by picosecond transient absorption. In this case, however, the complex does not function as a light–switch, actually exhibiting slightly enhanced luminescence upon binding to DNA. Furthermore, the Raman and electronic spectral evidence points to a lowest ^{3}MLCT excited state, which is tap$^{\bullet -}$ localized and to which electron transfer occurs from the guanine base of DNA. Investigations on these aspects continue [41].

3.4. Computational studies of $[Ru(L)_2dppz]^{2+}$

Recently, some theoretical investigations using density functional theory (DFT) have been initiated to investigate the nature of the intercalative interactions of the Ru^{II}dppz complexes with DNA. The first reported study [42] using INDO/SCF methods indicated that $[Ru\ (phen)_2dppz]^{2+}$ has a triplet state, at 2.06 eV, that is completely localized on the dppz ligand (i.e. ^{3}LC) and it was proposed that this state actually plays the role of the low-lying “dark” state of Ref. [16]. However, as the authors of the theoretical study themselves emphasise, in order to understand the nature of the excited states of the $[Ru(L)_2dppz]^{2+}$ species in solution, it is crucial to include in the calculations the effect of the solvent on the electronic structure, which was not technically feasible in that investigation. DFT/TDDFT calculations have also been reported for $[Ru(phen)_2dppz]^{2+}$ both in vacuo and in solution [43]. Further TDDFT investigations by the same authors provide additional insight into the nature of the excited states interacting with an adenine–thymine tetramer model system [44]. Another recent study [39] also points to solvent effects as critical for understanding the nature of the excitations. In this latter case it is concluded from the calculations that there exist two nearly degenerate triplet states in this molecule, one ligand based and one of MLCT character. It is proposed here also, as in the computational study referred to earlier [42], that the dark state is $^3\pi\pi^*$ in nature, as opposed to ^{3}MLCT. However this conclusion runs counter to both the luminescence [16,32] and transient resonance Raman [27,28,30,31,40] experimental evidence, all clearly in favor of MLCT character for both the D and B states of the light–switch.

4. Probing spin crossover (SCO) by Raman scatttering techniques

Since the first report of spin crossover behavior in Fe(III) by Cambi et al. in the early 1930s, [45] and Fe(II) complexes by Baker et al. [46] 30 years later, Fe(II) complexes have remained the centre of attention in the study of SCO behavior [3,47,48]. Several recent reviews of SCO behavior are already available in the literature and hence only representative aspects of SCO studies which have employed Raman spectroscopy as a probe will be discussed here [3,48].

The spin crossover effect is observed for complexes of transition metal ions, particularly of the first row, with electronic configurations between d^4 and d^7 and arises as a consequence of the splitting of the t_{2g} and e_g orbital sets [49]. The strength of the ligand field about the metal ion is a key (but not sole) factor, with weak and strong fields stabilizing high-spin (HS) and low-spin (LS) states, respectively. At intermediate field strengths the energy difference between the LS and HS states may be small enough that a change in the spin state, i.e a spin transition or spin crossover (SCO), may be brought about by means of an external perturbation involving for example a change in temperature, pressure or magnetic field or by irradiation with light.

For Fe(II) complexes, one of the effects of the spin crossover transition is that the formally anti-bonding e_g orbitals, unpopulated in the LS state are populated in the HS state. A lengthening and weakening of the Fe–L bond lengths accompanies the LS → HS transition, with a consequent change in the volume of the complex and its vibrational characteristics. In addition, changes in the visible spectroscopic and magnetic properties of the complex occur.

4.1. *Raman scattering as a spin-state specific probe—solid state studies*

The change in bond length, which accompanies SCO, is reflected in changes in the vibrational spectrum of the SCO complex. This makes vibrational spectroscopy, both infrared and Raman, particularly useful in providing fingerprints of the low and high spin states and as a means of following spin state changes. An additional attribute of Raman spectroscopy proves especially useful when visible lasers are used as excitation sources, enabling advantage to be taken of resonance enhancement of vibrational modes coupled to vibronic transitions resonant with the laser wavelength. A recent interesting example of this type, additionally noteworthy in being an an iron(III) SCO complex, is the study of [(TPA)Fe(III)(Cat)]BPh_4 (where TPA = tris(2-pyridylmethyl)amine and Cat = catecholate dianion), in which vibrational spectroscopy (resonance Raman and near-IR) in conjunction with other techniques was used to investigate the spin state transition between LS doublet and HS sextet states [50].

The purple-blue complex undergoes a two-step $S = \frac{1}{2} \to S = \frac{5}{2}$ spin-crossover in the solid state [51]. The X-ray crystal structure was solved at 110 and 220 K and shows a highly distorted pseudo-octahedral ferric complex that occupies two non-equivalent crystallographic sites. Variable temperature studies suggest that the two-step transition is due to the spin crossover process for each crystallographic site occurring at different temperatures.

Low temperature (15 K, λ_{exc} = 1064 nm) resonance Raman spectra indicate that the ground state of the complex in the low spin state possesses significant Fe(III)-catecholate and as well as Fe(II)-semiquinonate character (Fig. 12), an assignment supported by DFT calculations. Excitation of the complex at 270 K (λ_{ex} = 752.5 nm) shows features typical of a high spin complex. Surprisingly the resonance Raman spectrum obtained at 270 K remained unchanged (in terms of band shape and energy) down to 10 K. This persistence of the spectrum of the HS state at low temperatures, where only the LS form should be present, was attributed to at least two possible effects, laser-induced localized heating of the sample and light-induced excited spin-state trapping (LIESST—*vide infra*). Since the HS spectrum is so intense compared with the LS spectrum, even very small amounts of the complex present in the HS state due to such effects will swamp the LS signals. The findings underline the need for care in the interpretation of variable temperature Raman measurements in SCO systems in the solid state, where there is the risk of laser-generated local heating or LIESST effects. Even in such cases however, rR remains capable of providing useful structural information.

Another recent example of the application of Raman spectroscopy to the study of SCO behavior, is found in the study of the binuclear Fe(II) complex, $[\{Fe(NCBH_3)(4phpy)\}_2(\mu\text{-}bpypz)_2]$, where 4phpy = 2-phenylpyridine and bpypz = 3,5-bis(2′-pyridyl)-pyrazole, by Nakano et al. [52]. This complex exhibits a direct two-step LS/LS to HS/HS SCO process in the solid state. The Raman spectra of the singlet LS/LS state (at 100 K) and the HS/HS state at 296 K are combined in the spectrum recorded at 200 K indicating that the state at the plateau in the two-step spin crossover state is composed of 1:1 mixture of HS/HS and LS/LS rather than a mixed spin state (HS/LS).

Although the spin crossover phenomenon has been most commonly investigated as a function of temperature, the change in metal-ligand bond-lengths associated with the spin change and the concomitant volume change means that the spin state energy gap can also be influenced by the external pressure [53]. As with variable temperature studies, it is important in variable pressure SCO investigations to check that in the pressure range examined the structural integrity of the material is maintained and that morphological phase transitions do not occur.

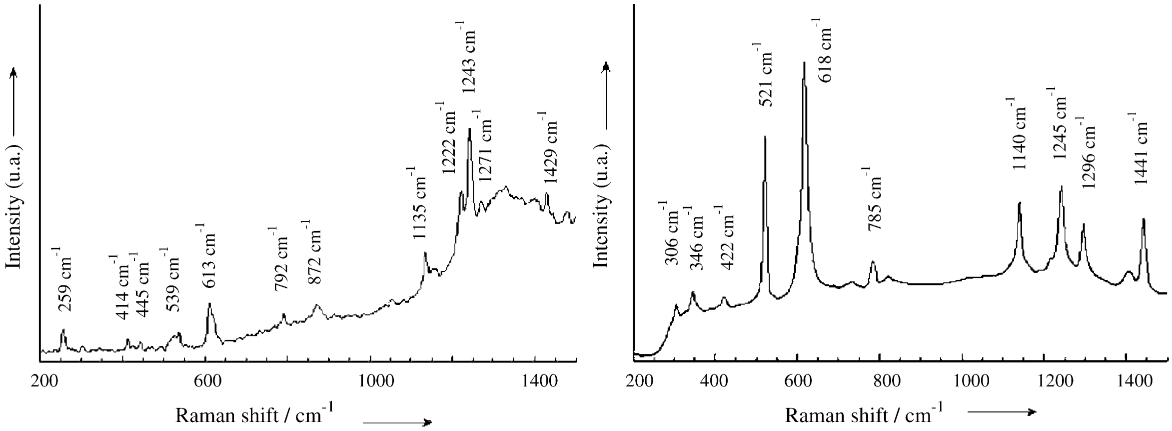

Fig. 12. RR spectrum of left; the LS form (15 K, 1064 nm excitation) and right; HS form of [(TPA)Fe(II)(Cat)]BPh$_4$ (270 K, 752.5 nm excitation). Reprinted with permission from Ref. [50]. Copyright [2005] John Wiley and Sons Inc.

The influence of external pressure on the SCO equilibrium has been investigated recently in the coordination polymers Fe(pyrazine)$_2$[M(CN)$_4$]·2H$_2$O (where M = Ni, Pd, Pt) which rather unusually exhibit SCO near room temperature, with T_c values (i.e. the temperatures marking equal HS and LS populations) in the region of 270–290 K [54]. In this series of complexes only the nickel(II) based polymer did not show competing pressure induced structural transformation. In addition, the nickel(II) based complex displayed a stable piezo-hysteresis loop [with spin transition pressures, $P_{1/2}\uparrow = 1350$ (±50) bar and $P_{1/2}\downarrow = 650$ (±50) bar], hence representing a rather unique example of a memory effect, brought about in this case by pressure [54]. The tunability of the SCO of this class of complexes was demonstrated in a subsequent investigation of the complex Fe(pyridine)$_2$[M(CN)$_4$] [55], which exhibited a spin transition at much higher pressure (11 kbar, Fig. 13). Notably, in this complex the Raman-active vibrational modes for both the LS and HS states were virtually pressure-independent in this pressure range. Raman scattering proved a particularly apt probe technique in these instances, because of its ability to 'track' even subtle changes in vibrational mode patterns as a function of pressure, enabling direct determination of the spin state of the material.

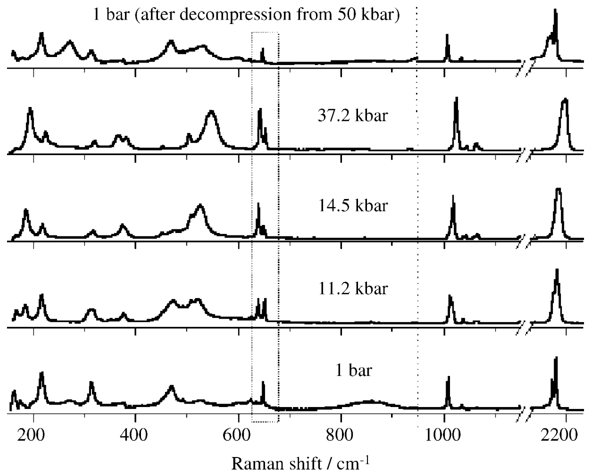

Fig. 13. Selected Raman spectra of Fe(pyridine)$_2$ [Ni(CN)$_4$] for different applied pressures at room temperature. Spectral intensities below 950 cm^{-1} are expanded by a factor of five. Reproduced with permission from Ref. [55]. Copyright The Institute of Physics [2004].

Recently Bonhommeau et al. have reported an example of the striking phenomenon of a reversible spin transition induced by a single laser pulse within the hysteresis loop in the SCO complex [Fe(C$_4$H$_4$N$_2$){Pt(CN)$_4$}] [56]. A light-induced spin transition within the hysteresis loop was actually first reported in a SCO complex (for the LS → HS direction only) using optical reflectivity as the probe [57]. However, in the more recent study [56], Raman spectroscopy enabled direct observation of both low and high spin states of the complex within the hysteresis loop, which in this instance occurred close to room temperature (Figs. 14 and 15).

The key empirical observation is that this phenomenon of reversible light-induced spin transition occurs only within the hysteresis loop and above and below this region normal photophysics and LIESST effects apply, i.e. excitation to the Franck-Condon state followed by ultrafast relaxation at 'high' temperatures (≥50 K), with LIESST occurring at cryogenic temperatures.

In solid samples co-operative effects between individual spin systems (metal centers) can have a large effect on the bulk SCO behavior of samples. Hysteresis effects in SCO solids have been linked to like-spin domain formation, with a nucleation-domain growth mechanism being important. In understanding the role of domains in the SCO behavior of solid samples, Raman spectroscopy has proven to be a useful tool. This is not only due to its sensitivity to subtle changes in vibrational structure but also on account of the possibility of using Raman microscopy to significantly enhance the degree of spatial resolution. This was exemplified in the micro-Raman mapping studies by Molnar et al. of the SCO complex, [Fe(pz)][Ni(CN)$_4$]·2H$_2$O, for which it was demonstrated that if like-spin domains do exist, their dimensions are likely to be sub-micron [58].

4.2. *Estimation of the vibrational contribution to the entropy change associated with spin crossover*

The LS → HS transition is an entropy-driven phenomenon. A key issue is the vibrational contribution to the total entropy

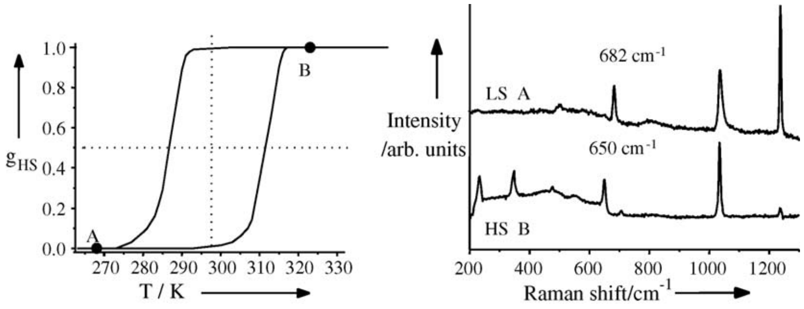

Fig. 14. Left: hysteresis loop for LS to HS transition; right: Raman spectra of the low and high spin states recorded at temperatures below (point A) and above (point B) the hysteresis loop. Reprinted with permission from Ref. [56]. Copyright [2005] John Wiley and Sons Inc.

change. The total is given by $\Delta S = R \ln(g_{HS}/g_{LS}) + \Delta S_{vib}$, where the first term is the electronic contribution arising from the degeneracies of the spin states ($g_{LS,HS} = 2S_{LS,HS} + 1$) and the second term is the vibrational part, $\Delta S_{vib}(\omega_i) = S_{HS}(\omega_i, T_c) - S_{LS}(\omega_i, T_c)$, where ω_i is the vibrational frequency of the ith vibrational mode and T_c is the temperature corresponding to equal LS, HS spin state populations, (i.e. $\Delta G(T_c) = 0$).

There has been a great deal of interest recently in using Raman spectroscopy in conjunction with other experimental and theoretical techniques (IR and nuclear inelastic scattering spectroscopy [59], X-ray crystallography and DFT) to quantify this contribution. Investigations on several systems have been reported, including $[Fe(phen)_2(NCS)_2]$, [60] the coordination polymers $Fe(pyridine)_2[M(CN)_4]$ (M = Pd, Pt)and $[Fe(pyrazine)[M(CN)_4]$ (M = Ni, Pd, Pt), [61] and the complex $\{FeL[H_2B(pz)_2]_3\}$ (L = phen or bpy) [62]. The general conclusion to emerge from the various investigations is that the major contribution to ΔS_{vib} originates in the Fe-ligand vibrations. However, in the case of the coordination polymeric systems, there were significant contributions also from other intra- and inter-molecular vibrational modes [61].

4.3. SCO in solution

Although the majority of SCO studies carried out have been concerned with the solid state, SCO transitions have been widely studied in solution also and this remains an important field of enquiry not least because studies in dilute solution enable the investigation of SCO in the absence of cooperative effects. Experimentally however, dilution of the SCO complex generally demands much higher detection sensitivity than required for solid materials. The differences in electronic structure between different spin states makes UV–vis absorption spectroscopy a method of choice for studying such systems. An example of the application of UV–vis spectroscopy in studying SCO relaxation behavior is found in the Fe(II) polypyridyl complex $Fe(btpa)](PF_6)_2$ (btpa = *N*,*N*,*N*′,*N*′-tetrakis(2-pyridylmethyl)-6,6′-bis(aminomethyl)-2,2′-bipyridine) [63]. From X-ray crystallographic studies the complex can exist as both a low spin hexacoordinate or a quasi-seven-coordinate high-spin complex [64].

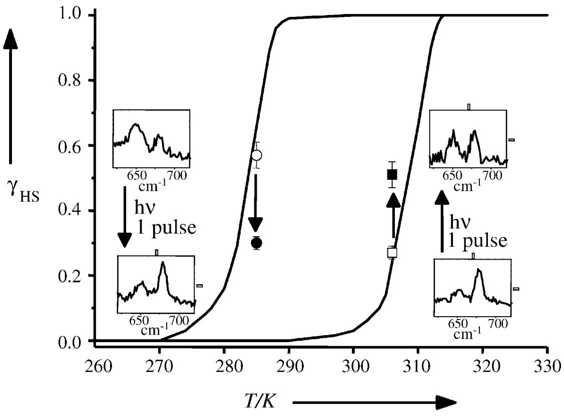

Fig. 15. Single shot laser induced spin state transition within the hysteresis loop. Reprinted with permission from Ref. [56] Copyright [2005] John Wiley and Sons Inc.

Photo-excitation of the ground state (^{1}A) of the complex in solution populates the HS (^{5}T) state. Using time-resolved resonance Raman spectroscopy, the relaxation dynamics of the complex in solution back to the ground state were monitored on both nanosecond and picosecond time scales. The use of a probe wavelength (321 nm), falling within the π–π^* transition of the polypyridyl backbone of the btpa ligand, enabled the study of vibrational modes of both LS and HS states (Fig. 16). The relaxation data from the nanosecond studies confirmed the earlier transient absorption spectrophotometric studies [64], pointing to biphasic spin-state relaxation of the complex $[Fe(btpa)](PF_6)_2$ in solution (upper plot, Fig. 17).

On the picosecond timescale, the TR^3 studies provided evidence that an early process, which is complete within 20 ps, involves vibrational relaxation of the $^5T_2$ state, whilst the nanosecond process corresponds to spin state relaxation from the thermally equilibrated HS (^{5}T) to the ground (LS, ^{1}A) state.

Light-induced spin crossover in an Fe(II) complex which is the experimental basis of the study just described was first reported in solution by McGarvey and Lawthers [65], The somewhat later report by Decurtins et al. of light-induced excited spin state trapping (LIESST) in the solid state [66] has led more recently to the emergence of several new effects including ligand-driven light-induced SCO [67–70], light-induced thermal hysteresis [71] and light-induced perturbation of a thermal hysteresis [72]. Recently Moussa et al. have reported LIESST and reverse LIESST effects in the SCO complex $[Fe(ptz)_6](BF_4)_2$, where ptz = 1-*n*-propyl-tetrazole [73]. In this complex, Raman spectroscopy provided evidence of both a spin state change

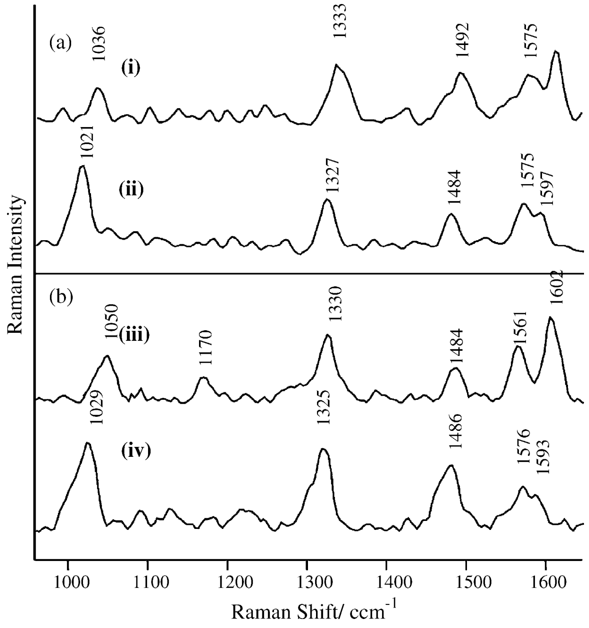

Fig. 16. Comparison of (a) representative (i) low-spin (LS) and (ii) high-spin (HS) spectra of [Fe(btpa)](PF$_6$)$_2$ obtained from subtractions of TR^3 spectra with (b) Raman spectra of “model” complexes, (iii) [Ru(btpa)](PF$_6$)$_2$ and (iv) [Zn(btpa)](PF$_6$)$_2$ obtained at 321 nm. Reprinted with permission from Ref. [64]. Copyright [2004] American Chemical Society.

and a crystallographic phase transition of the compound. The metastable HS state can be formed from the LS state at below 50 K by irradiation at 1342 nm and although thermal relaxation to the LS state occurs upon raising the sample temperature, a reverse LIESST effect can be induced by excitation into the HS $^5T_2$ to ^5E transition at 752.4 nm.

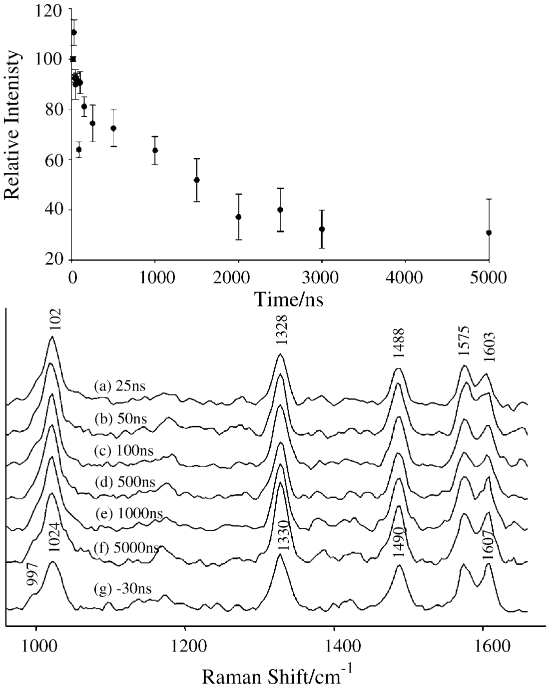

Fig. 17. Nanosecond-TR^3 study of [Fe(btpa)](PF$_6$)$_2$ in acetonitrile (concentration ca. 5×10^{-4} mol dm^{-3}; pump) 355 nm, 6 mJ; probe 321 nm, 0.65 mJ). Reprinted with permission from Ref. [64]. Copyright [2004] American Chemical Society.

5. Conclusions and outlook

Both types of metal-centered systems reviewed here represent convincing examples of the utility and potential of Raman and resonance Raman spectroscopy, both CW and time-resolved, for unraveling the often subtle interplay between the various factors (solvation, electronic character, etc.) controlling photophysics and excited state reactivity.

This is not to suggest that any single technique can be regarded as a universal problem solver across the broad area of transition metal photophysics and photochemistry. In the examples selected for discussion here it is clear that a judicious choice from a number of techniques still points the best way forward. The application of computational techniques to both light–switch and spin crossover phenomena, while obviously benefiting from recent advances in theory, is still in many respects in a developing phase, not least because of the necessity, in the case of comparison with studies in solution, to take full account of the effect of the solvent medium and, in the solid state, to allow for lattice effects [74].

References

[1] C. Creutz, M. Chou, T.L. Netzel, M. Okumura, N. Sutin, J. Am. Chem. Soc. 102 (1980) 1309.
[2] J.K. McCusker, Acc. Chem. Res. 36 (2003) 876.
[3] P. Gütlich, A. Hauser, H. Spiering, Angew. Chem. Int. Ed. 33 (1994) 2024.
[4] (a) K. Kalyanasundaram, Coord. Chem. Rev. 46 (1982) 159;
(b) J.M. Lehn, Angew. Chem., Int. Ed. Engl. 27 (1988) 89;
(c) V. Balzani, S. Campagna, G. Denti, A. Juris, S. Serroni, M. Ventura, Coord. Chem. Rev. 132 (1994) 1;
(d) V. Balzani, A. Juris, M. Venturi, S. Campagna, S. Serroni, Chem. Rev. 96 (1996) 759;
(e) V. Balzani, A. Juris, M. Venturi, S. Campagna, S. Serroni, Acc. Chem. Res. 31 (1998) 26;
(f) C.A. Slate, D.R. Striplin, J.A. Moss, P. Chen, B.W. Erickson, T.J. Meyer, J. Am. Chem. Soc. 120 (1998) 4885;
(g) Y.-Z. Hu, S. Tsukiji, S. Shinkai, S. Oishi, I. Hamachi, J. Am. Chem. Soc. 122 (2000) 241;
(h) J.-P. Sauvage, J.-P. Collin, J.-C. Chambron, S. Guillerez, C. Coudret, V. Balzani, F. Barigelletti, L. De Cola, L. Fannigni, Chem. Rev. 94 (1994) 993;
(i) J.N. Demas, B.A. DeGraff, Anal. Chem. 63 (1991) 829A.
[5] E.A. Seddon, K.R. Seddon, The Chemistry Of Ruthenium, Elsevier, Amsterdam, 1984 (Chapter 15).
[6] (a) V. Balzani, F. Scandola, Supramolecular Photochemistry, Ellis Horwood, Chichester, UK, 1991;
(b) V. Balzani (Ed.), Supramolecular Photochemistry, Reidel, Dordrecht, 1997;
(c) J.-M. Lehn, Supramolecular Chemistry, Wiley-VCH, Weinheim, 1995;
(d) A.K.D. Mesmacker, J.-P. Lecomte, J.M. Kelly, Top. Curr. Chem. 177 (1996) 25.
[7] (a) H. Dürr, S. Bossmann, Acc. Chem. Res. 34 (2001) 905;
(b) T.J. Meyer, Acc. Chem. Res. 22 (1989) 163;
(c) B. O'Regan, M. Graetzel, Nature 335 (1991) 737;
(d) L. De Cola, P. Belser, Coord. Chem. Rev. 177 (1998) 301;
(e) C.A. Bignozzi, J.R. Schoonover, F. Scandola, Progr. Inorg. Chem. 44 (1997) 1;

(f) M.-J. Blanco, M.C. Jiménez, J-C. Chambron, V. Heitz, M. Linke, J.-P. Sauvage, Chem. Soc. Rev. 28 (1999) 293;

(g) L. Sun, L. Hammarström, B. Åkermark, S. Styring, Chem. Soc. Rev. 30 (2001) 36;

(h) A. Magnunson, Y. Frapart, M. Abrahamsson, O. Horner, B. Åkermark, L. Sun, J.-J. Girerd, L. Hammarström, S. Styring, J. Am. Chem. Soc. 121 (1999) 89;

(i) J.-P. Collin, A. Harriman, V. Heitz, F. Odobel, J.-P. Sauvage, Coord. Chem. Rev. 148 (1996) 63.

[8] (a) S. McClanahan, T. Hayes, J. Kincaid, J. Am. Chem. Soc. 105 (1983) 4486;

(b) S.F. McClanahan, R.F. Dallinger, F.J. Holler, J.R. Kincaid, J. Am. Chem. Soc. 107 (1985) 4853;

(c) D.P. Strommen, P.K. Mallick, G.D. Danzer, R.S. Lumpkin, J.R. Kincaid, J. Phys. Chem. 94 (1990) 1357;

(d) G.D. Danzer, J.R. Kincaid, J. Phys. Chem. 94 (1990) 3976;

(e) S.M. Treffert-Ziemelis, J. Golus, D.P. Strommen, J.R. Kincaid, Inorg. Chem. 32 (1993) 3890.

[9] R.F. Dallinger, W.H. Woodruff, J. Am. Chem. Soc. 101 (1979) 4391.

[10] J.R. Schoonover, C.A. Bignozzi, T.J. Meyer, Coord. Chem. Rev. 165 (1997) 239.

[11] J.R. Schoonover, G.F. Strouse, Chem. Rev. 98 (1998) 1335.

[12] (a) K. Ronayne, PhD Thesis, Queen's University Belfast, Northern Ireland, 2004;

(b) K.F. Mongey, J.G. Vos, B.D. MacCraith, C.M. McDonagh, C. Coates, J.J. McGarvey, J. Mater. Chem. 7 (1997) 1473;

(c) C. Turro, S.H. Bossmann, G.E. Leroi, J.K. Barton, N.J. Turro, Inorg. Chem. 33 (1994) 1344.

[13] S.E.J. Bell, Analyst 121 (1996) 107R.

[14] W.R. Browne, N.M. O'Boyle, J.J. McGarvey, J.G. Vos, Chem. Soc. Rev. 34 (2005) 641.

[15] Z.J. Zhong, J.-Q. Tao, Z. Yu, C.-Y. Dun, Y.-J. Liu, X.-Z. You, C. J. Chem. Soc. Dalton Trans. (1998) 327.

[16] M.K. Brennaman, J.H. Alstrum-Acevedo, C.N. Fleming, P. Jang, T.J. Meyer, J.M. Papanikolas, J. Am. Chem. Soc. 124 (2002) 15094.

[17] (a) R.M. Hartshorn, J.K. Barton, J. Am. Chem. Soc. 114 (1992) 5919;

(b) Y. Jenkins, A.E. Friedman, N.J. Turro, J.K. Barton, Biochemistry 31 (1992) 10809;

(c) C.H. Hiort, P. Lincoln, B. Norden, J. Am. Chem. Soc. 115 (1993) 3448;

(d) L. Haq, P. Lincoln, D. Suh, B. Norden, B.Z. Chowdhry, J.B. Chaires, J. Am. Chem. Soc. 117 (1995) 4788.

[18] R.B. Nair, B.M. Cullum, C.J. Murphy, Inorg. Chem. 36 (1997) 962.

[19] J. Fees, W. Kaim, M. Moscherosch, W. Matheis, J. Klima, M. Krejcik, S. Zalis, Inorg. Chem. (1993) 166.

[20] E. Amouyal, A. Homsi, J.-C. Chambron, J.-P. Sauvage, J. Chem. Soc. Dalton Trans. (1990) 1841.

[21] J.R. Schoonover, W. Bates, T.J. Meyer, Inorg. Chem. 34 (1995) 6421.

[22] M.R. Waterland, K. Gordon, J. Raman Spectrom. 31 (2000) 243.

[23] M.R. Waterland, K.C. Gordon, J.J. McGarvey, P.M. Jayaweera, J. Chem. Soc. Dalton Trans. (1998) 609.

[24] M.K. Kuimova, W.Z. Alsindi, J. Dyer, D.C. Grills, O.S. Jina, P. Matousek, A.W. Parker, P. Portius, X.Z. Sun, M. Towrie, C. Wilson, J. Yang, M.W. George, Dalton. Trans. (2003) 3996.

[25] J. Dyer, W.J. Blau, C.G. Coates, C.M. Creely, J.D. Gavey, M.W. George, D.C. Grills, S. Hudson, J.M. Kelly, P. Matousek, J.J. McGarvey, J. McMaster, A.W. Parker, M. Towrie, J.A. Weinstein, Photochem. Photobiol. Sci. 2 (2003) 542.

[26] W. Chen, C. Turro, L.A. Friedman, J.K. Barton, N.J. Turro, J. Phys. Chem. B 101 (1997) 6995.

[27] C.G. Coates, L. Jacquet, J.J. McGarvey, S.E.J. Bell, A.H.R. Al-Obaidi, J.M. Kelly, Chem. Commun. (1996) 35.

[28] C.G. Coates, L. Jacquet, J.J. McGarvey, S.E.J. Bell, A.H.R. Al-Obaidi, J.M. Kelly, J. Am. Chem. Soc. 119 (1997) 7130.

[29] J.J. McGarvey, P. Callaghan, C.G. Coates, J.R. Schoonover, J.M. Kelly, L. Jacquet, K.C. Gordon, J. Phys. Chem. B 102 (1998) 5941.

[30] C.G. Coates, J. Olofsson, M. Coletti, J.J. McGarvey, B. Onfelt, P. Lincoln, B. Norden, E. Tuite, P. Matousek, A.W. Parker, J. Phys. Chem. 105 (2001) 12653.

[31] J. Olofsson, B. Onfelt, P. Lincoln, B. Norden, P. Matousek, A.W. Parker, E. Tuite, J. Inorg. Biochem. 91 (2002) 286.

[32] M.K. Brennaman, T.J. Meyer, J.M. Papanikolas, J. Phys. Chem. A 108 (2004) 9938.

[33] E.J.C. Olson, D. Hu, A. Hörmann, A.M. Jonkman, M.R. Arkin, E.D.A. Stemp, J.K. Barton, P.F. Barbara, J. Am. Chem. Soc. 119 (1997) 11458.

[34] R.B. Nair, B.M. Cullum, C.J. Murphy, Inorg. Chem. 36 (1997) 962.

[35] A.C. Benniston, P. Matousek, A.W. Parker, J. Raman Spectrosc. 31 (2000) 503.

[36] B. Onfelt, J. Olofsson, P. Lincoln, B. Norden, J. Phys. Chem. A 107 (2003) 1000.

[37] J. Olofsson, B. Onfelt, P. Lincoln, J. Phys. Chem. A 108 (2004) 4391.

[38] C.G. Coates, P.L. Callaghan, J.J. McGarvey, J.M. Kelly, P.E. Kruger, M.E. Higgins, J. Raman Spectrosc. 31 (2000) 283.

[39] E.R. Batista, R.L. Martin, J. Phys. Chem. A 109 (2005) 3128.

[40] C.G. Coates, P. Callaghan, J.J. McGarvey, J.M. Kelly, L. Jacquet, A. Kirsch-De Mesmaeker, J. Mol. Struct. 598 (2001) 15.

[41] I. Ortmans, B. Elias, J.M. Kelly, C. Moucheron, A. Kirsch-DeMesmaeker, Dalton Trans. (2004) 668.

[42] G. Pourtois, D. Beljonne, C. Moucheron, S. Schumm, A. Kirsch-de Mesmaeker, R. Lazzaroni, J.-L. Bredas, J. Am. Chem. Soc. 126 (2004) 683.

[43] S. Fantacci, F. De Angelis, A. Sgamellotti, N. Re, Chem. Phys. Lett. 396 (2004) 43.

[44] S. Fantacci, F. De Angelis, A. Sgamellotti, M. Alessandro, N. Re, J. Am. Chem. Soc. 127 (2005) 14144.

[45] (a) L. Cambi, A. Cagnasso, Atti Accad. Naz. Lincei 13 (1931) 809;

(b) L. Cambi, L. Szegö, A. Cassano, Atti Acad. Naz. Lincei 15 (1932) 329.

[46] W.A. Baker, H.M. Bobonich, Inorg. Chem. 3 (1964) 1184.

[47] J.K. Beattie, Adv. Inorg. Chem. 32 (1988) 1.

[48] (a) C. Brady, J.J. McGarvey, J.K. McCusker, H. Toftlund, D.N. Hendrickson, in: P. Gütlich, H.A. Goodwin (Eds.), Spin Crossover in Transition Metal Compounds III, Top. Curr. Chem. 235 (2004) 1;

(b) P. Gütlich, Y. Garcia, H.A. Goodwin, Chem. Soc. Rev. 29 (2000) 419;

(c) H. Toftlund, Coord. Chem. Rev. 94 (1989) 67.

[49] The term symbols t_{2g} and e_g refer to an octahedral symmetry, which is seldom the case for spin crossover complexes, however the symbols are used for convenience.

[50] A.J. Simaan, M-L. Boillot, R. Carrasco, J. Cano, J-J. Girerd, T.A. Mattioli, J. Ensling, H. Spiering, P. Gütlich, Chem. Euro. J. 11 (2005) 1779.

[51] A.J. Simaan, M.-L. Boillot, E. Rivire, A. Boussac, J.-J. Girerd, Angew. Chem. Int. Ed. 39 (2000) 196.

[52] K. Nakano, S. Kawata, K. Yoneda, A. Fuyuhiro, T. Yagi, S. Nasu, S. Morimoto, Kaizaki, Chem. Commun. (2004) 2892.

[53] For recent reviews see:

(a) A. Bousseksou, G. Molnar, G. Matouzenko, Eur. J. Inorg. Chem. (2004) 4353;

(b) P. Gutlich, V. Ksenofontov, A.B. Gaspar, Coord. Chem Rev. 249 (2005) 1811.

[54] G. Molnar, V. Niel, J.-A. Real, L. Dubrovinsky, A. Bousseksou, J.J. McGarvey, J. Phys. Chem. B 107 (2003) 3149.

[55] G. Molnar, T. Kitazawa, L. Dubrovinsky, J.J. McGarvey, A. Bousseksou, J. Phys. Condens. Matter. 16 (2004) 1129.

[56] S. Bonhommeau, G. Molnar, A. Galet, A. Zwick, J.-A. Real, J.J. McGarvey, A. Bousseksou, Angew. Chem. Int. Ed. Engl. 44 (2005) 4069.

[57] E. Freysz, S. Montant, S. Letard, J.-F. Letard, Chem. Phys. Lett. 394 (2004) 318.

[58] G. Molnar, A. Bousseksou, A. Zwick, J.J. McGarvey, Chem. Phys. Lett. 367 (2002) 593.

[59] H. Paulsen, V. Schunemann, A.X. Trautwein, H. Winkler, Coord. Chem. Rev. 249 (2005) 255.

[60] (a) A. Bousseksou, J.J. McGarvey, F. Varret, J.A. Real, J.-P. Tuchagues, A.C. Dennis, M.L. Boillot, Chem. Phys. Lett. 318 (2000) 409;

(b) G. Brehm, M. Reiher, S. Schneider, J. Phys. Chem. A 106 (2002) 12024.
[61] G. Molnar, V. Niel, A.B. Gaspar, J.-A. Real, A. Zwick, A. Bousseksou, J.J. McGarvey, J. Phys. Chem. B 106 (2002) 9701.
[62] N. Moliner, L. Salmon, L. Capes, M.C. Munoz, J.-F. Letard, A. Bousseksou, J.-P. Tuchagues, J.J. McGarvey, A.C. Dennis, M. Castro, R. Burriel, J-A. Real, J. Phys. Chem. B 106 (2002) 4276.
[63] S. Schenker, P.C. Stein, J.A. Wolny, C. Brady, J.J. McGarvey, H. Toftlund, A. Hauser, Inorg. Chem. 40 (2001) 134.
[64] C. Brady, P.L. Callaghan, Z. Ciunik, C.G. Coates, A. Dossing, A. Hazell, J.J. McGarvey, S. Schenker, H. Toftlund, A.X. Trautwein, H. Winkler, J.A. Wolny, Inorg. Chem. 43 (2004) 4289.
[65] J.J. McGarvey, I. Lawthers, J. Chem. Soc. Chem. Commun. (1982) 906.
[66] S. Decurtins, P. Gütlich, C.P. Köhler, H. Spiering, A. Hauser, Chem. Phys. Lett. 105 (1984) 1.
[67] (a) J. Zarembowitch, C. Roux, M.-L. Boillot, R. Claude, J.-P. Itie, A. Polian, M. Bolte, Mol. Cryst. Liq. Cryst. 234 (1993) 247;
(b) C. Roux, J. Zarembowitch, B. Gallois, T. Granier, R. Claude, Inorg. Chem. 33 (1994) 2273.
[68] M.-L. Boillot, S. Chantraine, J. Zarembowitch, J.-Y. Lallemand, J. Prunet, New J. Chem. (1999) 179.
[69] A. Sour, M.-L. Boillot, E. Riviere, P. Lesot, Eur. J. Inorg. Chem. (1999) 2117.
[70] S. Hayami, Z.Z. Gu, Y. Einaga, Y. Kobayasi, Y. Ishikawa, Y. Yamada, A. Fujishima, O. Sato, Inorg. Chem. 40 (2001) 3240.
[71] A. Desaix, O. Roubeau, J. Jeftic, J.G. Haasnoot, K. Boukheddaden, E. Codjovi, J. Linares, M. Nogues, F. Varret, Eur. Phys. B 6 (1998) 183.
[72] F. Renz, H. Spiering, H.A. Goodwin, P. Gütlich, Hyperfine Interact. 126 (2000) 155.
[73] N.O. Moussa, G. Molnar, X. Ducros, A. Zwick, T. Tayagaki, K. Tanaka, A. Bousseksou, Chem. Phys. Lett. 402 (2005) 503.
[74] H. Paulsen, A.X. Trautwein, Topics Curr. Chem. 235 (2004) 197.